applied sciences

MDPI

Perspective

Graphene-Based Membranes for CO_2/CH_4 Separation: Key Challenges and Perspectives

Kunli Goh [1,2,*], H. Enis Karahan [1,2], Euntae Yang [1,2] and Tae-Hyun Bae [3]

[1] Singapore Membrane Technology Center, Nanyang Technological University, Singapore 637141, Singapore
[2] School of Chemical and Biomedical Engineering, Nanyang Technological University, Singapore 637459, Singapore
[3] Department of Chemical and Biomedical Engineering, Korea Advanced Institute of Science and Technology (KAIST), Daejeon 305-338, Korea
* Correspondence: gohkunli@ntu.edu.sg; Tel.: +65-6592-1664

Received: 10 June 2019; Accepted: 8 July 2019; Published: 10 July 2019

Abstract: Increasing demand to strengthen energy security has increased the importance of natural gas sweetening and biogas upgrading processes. Membrane-based separation of carbon dioxide (CO_2) and methane (CH_4) is a relatively newer technology, which offers several competitive advantages, such as higher energy-efficiency and cost-effectiveness, over conventional technologies. Recently, the use of graphene-based materials to elevate the performance of polymeric membranes have attracted immense attention. Herein, we do not seek to provide the reader with a comprehensive review of this topic but rather highlight the key challenges and our perspectives going ahead. We approach the topic by evaluating three mainstream membrane designs using graphene-based materials: (1) nanoporous single-layer graphene, (2) few- to multi-layered graphene-based stacked laminates, and (3) mixed-matrix membranes. At present, each design faces different challenges, including low scalability, high production cost, limited performance enhancement, and the lack of robust techno-economic review and systematic membrane design optimization. To help address these challenges, we have mapped out a technology landscape of the current graphene-based membrane research based on the separation performance enhancement, commercial viability, and production cost. Accordingly, we contend that future efforts devoted to advancing graphene-based membranes must be matched by progress in these strategic areas so as to realize practical and commercially relevant graphene-based membranes for CO_2/CH_4 separation and beyond.

Keywords: graphene-based material; CO_2 separation; mixed-matrix membrane; F_{index}; Robeson upper bound; graphene-based laminate; single-layer graphene

1. Introduction

The strong demand for energy to meet the increasing population and economic growth has motivated a shift towards alternative energy resources to supplement the depleting conventional fossil fuels [1]. Such a change is also driven by the escalating environmental and public health issues associated with the anthropogenic climate change [2,3]. As a result, methane gas (CH_4) attracts an immense amount of attention as it is a relatively cleaner form of fuel with a lower carbon per unit energy as compared to other fossil fuels. Moreover, there is an abundant amount of CH_4 in the form of natural gas, and sustainable supplies of biogas also make CH_4 a good choice of renewable energy [4,5]. Typically, natural gas and biogas can contain up to 90% CH_4 with up to 50% carbon dioxide gas (CO_2) [4]. To increase the calorific value and marketability of natural gas and biogas, there is a need to sweeten and enrich the amount of CH_4 in them. CO_2/CH_4 separation, therefore, becomes an important application.

Conventionally, CO_2/CH_4 separation has been carried out using chemical and water scrubbing, adsorption processes and cryogenic distillation [6]. Membrane-based CO_2/CH_4 separation is a relatively newer technology which boasts higher energy-efficiency and cost-effectiveness, as well as a more robust design with a smaller plant footprint [5,7]. Hence, membrane separation is a promising technology to realize high-performance CO_2/CH_4 separation. To achieve this vision, advanced membranes using state-of-the-art materials are necessary [8]. Recently, graphene-based materials have been showcased as an attractive material for membrane preparation, owing to their two-dimensional (2D) morphology and tunable physicochemical properties [9]. In particular, the monoatomic thickness of graphene-based materials gives theoretically the lowest transport resistance possible of a membrane [10] and their rich chemistry enables tailorable chemical functionalization to suit the needs of different membrane-based applications [9,11]. Among the different graphene-based materials exploited thus far, graphene oxide (GO) shows exceptional hydrophilicity, as well as water solubility [12]. Thus, the competitive advantage of GO lies in its solution processability, which allows easy processing into continuous films [13], and seamless integration with existing membrane fabrication techniques [11]. For this reason, GO garners widespread attention from the membrane community and is one of the most extensively used graphene-based materials for designing membranes to date.

In this paper, we do not seek to furnish the reader with a comprehensive overview of graphene-based membranes for CO_2/CH_4 separation since several high-quality reviews are already available in the literature [9,11,14–18]. Rather, we aim to arouse awareness of various challenges faced by current graphene-based membranes for CO_2/CH_4 separation. By doing so, we hope to kindle the interest of researchers by sharing solution-oriented perspectives that can potentially put together effective strategies for resolving these challenges. As such, we initiate our discussion from three mainstream graphene-based membrane designs, namely, (1) nanoporous single-layer graphene; (2) few- to multi-layer graphene-based stacked laminate and (3) mixed-matrix membrane (Figure 1). We first present a brief review summarizing the current progress to help the reader grasps the essential background of this research field, before proceeding to focus on several key challenges for each membrane design. The discussion then closes off with useful insights from positive implementation in practice or problem-solving strategies that can be prospective solutions to help advance graphene-based membranes for CO_2/CH_4 separation. Beyond CO_2/CH_4 separation, these insights are also of relevance to a wider community with interests in other gas separation and water treatment applications.

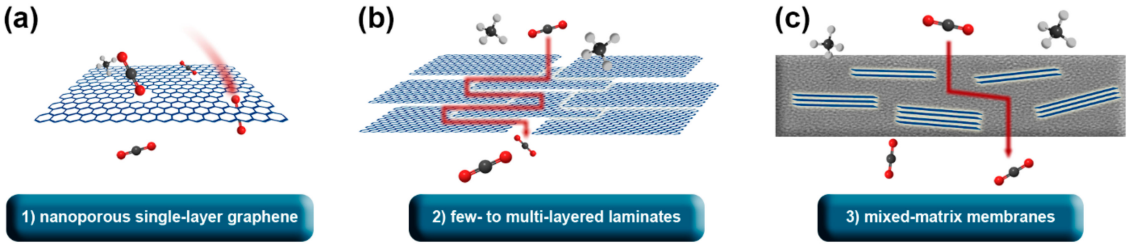

Figure 1. Three mainstream graphene-based membrane designs, namely, (**a**) nanoporous single-layer graphene, (**b**) few- to multi-layer stacked laminate, and (**c**) mixed-matrix membrane, which is the focus of this article.

2. Nanoporous Singe-Layer Graphene

A defect-free single-layer graphene nanosheet is impermeable to gas molecules [19,20]. To enable single-layer graphene as a membrane, there is a need to generate nanopores of optimized pore size for separation by a molecular sieving mechanism. The kinetic diameters of CO_2 and CH_4 molecules are 3.30 and 3.82 Å, respectively [5]. In this context, therefore, it implies that the ideal pore size of single-layer graphene membrane should be between these kinetic diameters so that CO_2 molecules are allowed to permeate through, while the CH_4 molecules are retained. There are several etching techniques used to

generate nanopores on single-layer graphene nanosheet to date, including ion bombardment followed by chemical oxidation [21], focus-ion beam (FIB) patterning [10], gold nanoparticle deposition followed by oxidation [22], oxygen plasma [23] with ozone etching [24], and ultraviolet-induced oxidative treatment [25]. Each method utilizes etching to first create defects on the pristine single-layer graphene which can then be aggravated into nanopores. There appears no systematic control over the pores sizes by using different techniques. For example, Koenig et al. generated subnanometer pores of size 3.4 to 5 Å using ultraviolet-induced oxidative treatment to obtain high ideal CO_2/CH_4 selectivity at 9.0×10^3 [25]. Celebi et al. used an FIB patterning method to create pores that were in the range of 7.6 to 1000 nm, which showed the highest H_2/CO_2 mixed gas selectivity of 3.4 using the graphene membrane containing 7.6 nm pores [10].

2.1. Challenges

The greatest advantage of nanoporous single-layer graphene lies in the monoatomic thickness, which conceptually exerts the lowest membrane resistance and possesses the greatest potential for achieving high CO_2 permeability [10]. However, freestanding nanoporous single-layer graphene is not capable of serving as a functional membrane owing to its insufficient mechanical properties. Apart from that, nanoporous single-layer graphene membranes are not readily scalable. Single-layer graphene is normally produced by a chemical vapor deposition (CVD) method with a surface area that is too small [11]. Furthermore, pore generation using the aforementioned techniques remain difficult to control, making uniform pore size generation and narrow pore size distribution not easily realizable. To enable nanoporous single-layer graphene as a functional membrane, the most feasible approach is to adopt a composite membrane design where the single-layer graphene layer first undergoes treatment to form nanopores before transferring to the top of a porous polymer substrate as the selective layer (Figure 2a). In this regard, large-scale and defect-free transfer of the nanoporous single-layer graphene onto the polymer substrate is yet another challenge to consider.

2.2. Perspectives

Ensuring a uniform pore size generation and narrow pore size distribution appears to be the bottleneck towards synthesizing functional nanoporous single-layer graphene membrane for CO_2/CH_4 separation. This is because all the etching techniques that have been developed so far occur in a random manner with no means to provide atomic-level control of where the etching takes place. Hence, future research direction should gear towards finding more controllable means of creating nanopores on single-layer graphene. Alternatively, rather than a top-down effort, a bottom-up approach can also be used to generate uniform nanopores through structural manipulations. For example, it is possible to synthesize graphene-like nanosheets, such as graphyne and graphdiyne materials, for gas separation applications [26]. Graphyne and graphdiyne are carbon allotropes comprising both hexagonal rings and acetylenic linkages made up of sp- and sp^2-hybridized carbon atoms [27]. Like graphene-based materials, they possess a 2D morphological network. Yet, the key attribute is not in the 2D network but their uniformly distributed pores (Figure 2b,c), which is something lacking in pristine graphene nanosheets [27,28]. Owing to these intrinsic pores, γ-graphdiyne is regarded as highly attractive as it has been shown through molecular dynamic simulations to possess gas separation properties that are way better than graphene [28,29]. However, one potential trade-off is the challenge in synthesizing monolayer highly-crystalline γ-graphdiyne with a reasonably large surface area for evaluation by gas separation microdevices. This feat is to date more challenging to achieve than single-layer graphene, especially since the growth mechanism of graphyne and graphdiyne materials has yet to be fully understood [28].

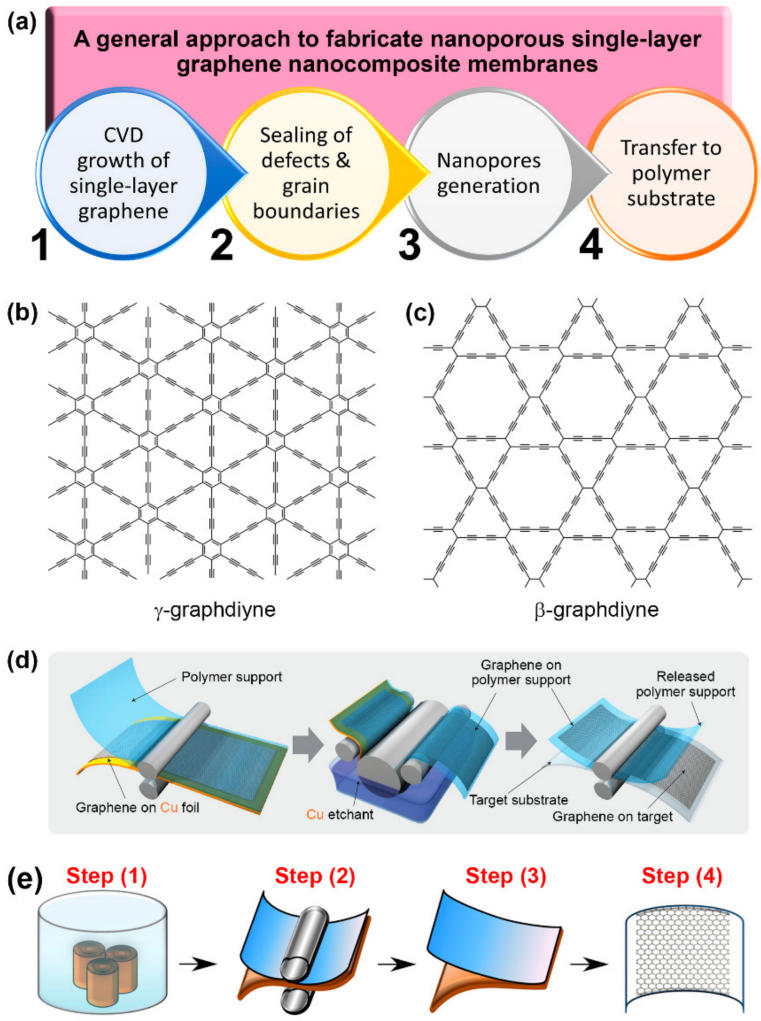

Figure 2. (**a**) Schematic showing a general approach to synthesizing nanoporous single-layer nanocomposite graphene membrane. Chemical structures of (**b**) γ- and (**c**) β-graphdiyne. (**d**) A typical roll-to-roll-based production of large-area single-layer graphene on a target substrate. Adapted from Reference [30]. (**e**) A typical large-area single-layer graphene transfer using a hot-roll laminate: (1) copper foil oxidized in deionized water for overnight, (2) the oxidized foil laminated with a commercial polyvinyl alcohol (PVA) film using a hot-roll laminator, (3) the PVA film mechanically delaminated from the copper foil after baking at 110 °C, and (4) the ensuing large-area single-layer graphene transferred on the PVA film. Adapted from Reference [31]. Creative Commons license CC BY 4.0.

Comparatively, the progress made in large-scale synthesis and defect-free transfer of single-layer graphene appears to show greater promise. Roll-to-roll-based production of graphene synthesis and transfer had already been demonstrated, which was able to give up to 30-inch of high-quality single-layer graphene film on a polyethylene terephthalate (PET) substrate (Figure 2d) [30]. Recently, nondestructive large-area single-layer graphene transfer had also advanced to a stage where it can be done using a simple hot-roll laminator, making the overall transfer more effective, less complex, and easily adoptable for industrial applications (Figure 2e) [31]. Still, the question remains on how to incorporate the prior steps of defects and grain boundary sealing and nanopores generation before this graphene transfer step (Figure 2a) to realize a single and continuous line that is more suited for industrial production.

3. Few- to Multi-Layer Graphene-Based Stacked Laminates

Relative to the single-layer graphene membrane, the few- to multi-layer stacked graphene-based laminates, with more than one layer of nanosheet, can easily form a continuous film. The requirement on the quality and integrity of the nanosheets is, therefore, less stringent for this type of membrane design. Hence, there is no need for an elaborated bottom-up CVD synthesis to obtain high-quality graphene. Instead, membranes with few- to multi-layer stacked graphene-based laminates are usually prepared from a top-down approach, mostly using graphene oxide (GO) nanosheets that are derived from the oxidation of graphite. GO nanosheets are by far the most commonly used graphene-based material for preparing stacked laminates, owing to their facile synthesis and rich surface chemistry arising from oxygen-containing functional groups, such as the hydroxyl, carboxyl, and epoxy groups [5,9]. More importantly, GO nanosheets are highly water-soluble, making them solution processable and easy for membrane fabrications [11]. To date, GO-based stacked laminates are generally fabricated from a myriad of techniques, such as vacuum-assisted filtration [32,33], pressure-assisted filtration [13,34], spin-coating [35,36], spray-coating [37], dip-coating [12], shear-alignment [38], and layer-by-layer (LbL) techniques [39].

GO-based stacked laminates can range from a thickness of 1.8 nm (~3 layers of GO nanosheets) to several micrometers (multi-layered) [13,32]. The ideal thickness of the laminates depends on the gas pairs to be separated and the target applications. For example, Li et al. prepared an ultrathin GO laminated membrane of 1.8 nm in thickness for selective hydrogen separation. The study, however, demonstrated a rather anomalous result where CO_2 permeance was reportedly lower than that of CH_4, making the membrane irrelevant for CO_2/CH_4 separation [32]. In another work, Kim et al. synthesized a slightly thicker membrane at ~3 nm for CO_2 separation. The results showed CO_2 as the more permeable gas with an intrinsic permeability of ~8500 barrer and CO_2/CH_4 selectivity of ~10 [36]. As the thickness continues to increase to the micrometer scale, GO laminates also evolve from a selective membrane into a gas-diffusion barrier where O_2 permeability can even reach lower than 0.01 barrer [19]. Such gas-diffusion barriers usually find applications in food packaging and electronic devices [13,19]. The transport mechanism behind these stacked laminates stems from the tortuous diffusion pathways that gas molecules have to take in order to permeate through the laminates (Figure 3a). Undoubtedly, the most immediate impact is on the gas permeability. This is because the transport mechanism through the laminate is more often than not governed by a solution-diffusion mechanism where permeability is a function of solubility and diffusivity. As the thickness of the laminates increases, the diffusion pathway gets longer and more extended. For this reason, CO_2 diffusivity decreases and the difference in solubility and diffusivity between CO_2 and CH_4 is magnified. The CO_2/CH_4 selectivity, therefore, gets elevated but at the expense of the CO_2 permeability.

The thickness of GO-based stacked laminates is one of the most crucial criteria for making a defect-free continuous film. In this regard, thicker laminates are better as they are not only more processable from the membrane fabrication standpoint but defects arising from incomplete coverage of GO nanosheets can be rectified by increasing the thickness. Also, thicker laminates are easier to handle and manage. Hence, GO-based stacked laminates can be readily adopted as barrier films. For application as selective membranes, the use of thicker laminates is usually accompanied by a compromised gas permeability, including CO_2. Researchers have sought several strategies to overcome this drawback, which include using porous (holey) graphene nanosheets to facilitate a more direct CO_2 transport (Figure 3b), chemical functionalization to increase the affinity for CO_2 (Figure 3c) and intercalation by spacers to increase the interlayer spacing between the GO nanosheets (Figure 3d) [5,40,41]. To this end, the most commonly used spacers include ionic liquids, various ions (such as metal and borate ions), as well as a multitude of CO_2-philic amine-based crosslinkers [5,33,42–44].

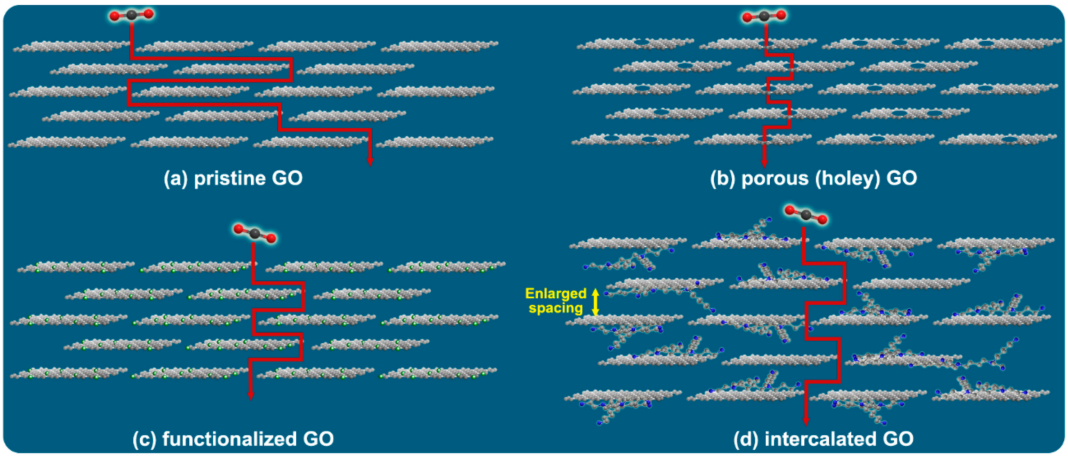

Figure 3. Graphene-based stacked laminates as membranes using (**a**) pristine graphene oxide (GO) nanosheets with an extensive and tortuous diffusion pathway, (**b**) porous (holey) GO nanosheets with a more direct carbon dioxide (CO_2) transport through the pores, (**c**) chemically functionalized GO nanosheets with a stronger affinity towards CO_2 molecules, leading to a facilitated transport, and (**d**) intercalated GO nanosheets with enlarged interlayer spacing and lower membrane resistance for CO_2 diffusion.

3.1. Challenges

Currently, commercial polymeric membranes for CO_2/CH_4 separation comes in two configurations: (1) flat-sheet in spiral-wound membrane modules, and (2) hollow fiber in hollow fiber membrane modules. Spiral wound modules based on cellulose acetate flat-sheet membranes from UOP Separex™ have been around for more than 25 years, while other companies, such as Cameron and Ube Industries in Japan, produce cellulose triacetate and polyimide hollow fiber membranes, respectively, for CO_2/CH_4 separation [45]. Hollow fibers membranes are widely used for industrial gas separation membranes [15], especially for high-pressure separation, such as natural gas sweetening, owing to their high packing density, large membrane surface area per module and relatively lower module production costs [46]. On the other hand, spiral-wound flat-sheet membranes are more commonly used in low-pressure or vacuum-driven gas separation [46]. However, to date, GO-based stacked laminates are only often demonstrated as flat-sheet membranes with reason plausibly attributed to the ease of membrane fabrications and performance evaluations. Reports on GO-based stacked laminates are, in comparison, more limited. Hence, there exists a gap between current academic pursue and industrial needs, making technology transfer and commercialization less straightforward. Owing to the large membrane surface area particularly for hollow fiber membranes, a larger quantity of graphene-based materials is also needed to produce GO- or graphene-based stacked laminates at a mass production level. This means that the cost of producing GO-based stacked laminates as gas separation membranes will become less competitive. While we foresee that the production cost is much lower than nanoporous single-layer CVD graphene membranes, it is likely to stay higher as compared to the mixed-matrix membrane design and definitely more costly than current polymeric membranes [11]. The question, therefore, lies in whether the higher CO_2/CH_4 separation performances are worth the additional capital investment on these graphene-based laminates.

3.2. Perspectives

To fill the technological gap, we contend that research efforts should focus on graphene-based stacked laminates that have greater potential for practical large-scale membrane applications. Specifically, graphene-based stacked laminates with good scalability and processability must be given closer attention. These include flat-sheet graphene-based stacked laminates that are prepared by shear-alignment (or commonly known as doctor-blade technique) and spray-coating techniques,

as well as dip-coated hollow fiber graphene-based stacked laminates. As compared to vacuum- and pressure-assisted filtration techniques which are widely adopted by the academia, stacked laminates prepared from these techniques have greater relevance as they are more commonly used by the membrane industry. Hence, to ensure effective implementation of graphene-based stacked laminates, we propose to strengthen the efforts in the following five key initiatives. First, future endeavors should move from current lab-scale prototypes to large-scale demonstrations. In recent years, GO-based stacked laminates fabrications are progressively moving from tenth to thousandth of square centimeters by using the aforementioned techniques [11,13,38,47]. This looks promising given that the current scale of effective membrane area is now able to support pilot-plant studies. Second, with successful large-scale demonstrations, the stacked laminate membrane design must then be optimized to maximize its CO_2/CH_4 separation performances. This includes optimizing the lateral dimension of the graphene-based materials used, the thickness of the laminates, as well as the choice of substrates. Also, for laminates which utilized chemical functionalization and spacer intercalation to enhance the CO_2 permeability, it is necessary to optimize the extent of functionalization and loading of the intercalated spacers to tune the interlayer spacing between the graphene sheets, as well as for processability of the laminates and defect control. Third, creating a deeper understanding of the membrane stability and long-term separation performances of graphene-based stacked laminates is critical. In particular, biogas and natural gas contain water vapor and impurity gases, such as H_2S [4,48]. As such, we expect graphene-based stacked laminates, especially the GO-based ones, to show detrimental effects on the long-term stability given that the oxygen-containing functional groups can interact readily with the water vapor and H_2S to induce competitive sorption and plasticization effect [16,49]. Fourth, developing more effective techniques to realize hollow fiber graphene-based stacked laminates will be instrumental in improving the marketability and adoption of the membranes for CO_2/CH_4 separation. Last but not least, there is a need to retrofit graphene-based stacked laminates processing into existing polymeric membrane fabrication manufacturing to produce a continuous production line. Without progress made in any of these initiatives, graphene-based stacked laminates for CO_2/CH_4 separation is likely to receive poor commercial acceptance by the industry.

Beyond the technological aspects, increasing efforts to provide comprehensive techno-economic analyses of graphene-based stacked laminates are absolutely essential. This is because, despite the higher CO_2/CH_4 separation performances offered by the stacked laminates, they come at an extra cost. Hence, it is necessary to further ascertain the true impact of using graphene-based stacked laminates both from the process design and return on investment perspective. For example, Baker proposed that if the membrane performance was raised to a CO_2 permeance of 100 GPU and CO_2/CH_4 selectivity of 40 as compared to the ~50 GPU and ~15 selectivity of current standard cellulose acetate membrane, it is hypothetically feasible to achieve a reduction in the membrane area, compressor loading, and CH_4 loss through the permeate of up to 75%, which can potentially be translated to savings in the process design [50]. Further, Scholz analyzed that it is possible to create a higher annual profit and lower upgrading cost by using a high-performance membrane for a biogas upgrading plant of capacity 150 N m^3 h^{-1}. Specifically, an annual profit increment and upgrading cost savings of 8% and 86%, respectively, can be expected when membrane selectivity increased from 20 to 60, assuming the same CO_2 permeance of 60 GPU [51]. To date, such techno-economic studies on graphene-based stacked laminates are rather limited. It is, therefore, very difficult to judge the true potential of graphene-based stacked laminates for CO_2/CH_4 separation just by considering the high separation performances.

4. Mixed-Matrix Membranes

Among the different types of graphene-based membranes for CO_2/CH_4 separation discussed herein, the mixed-matrix membrane design is the most functional and possesses the greatest commercial potential [52]. Mixed-matrix membranes are defined when a solid phase filler material is added into a continuous matrix of polymer phase [53]. In this context, the graphene-based materials serve as the filler materials. The rationale of doing so is to utilize the key attributes of the graphene-based

materials to engineer the transport properties of the polymer matrix. As already mentioned in the Introduction, the key attributes of graphene-based materials are their 2D morphologies and tunable physicochemical properties.

The role of graphene-based materials in a mixed-matrix design is slightly different from the stacked laminates. At low loadings, the graphene-based materials capitalize on their well-defined interlayer spacing as low resistance nanochannels for diffusion of the smaller CO_2 molecules. Comparatively, the slightly larger CH_4 molecules are unable to gain access into the interlayer spacing and are forced to diffuse around the graphene-based fillers and through the polymer matrix with higher transport resistance (Figure 4a). For example, Shen et al. prepared a polyether block amide (PEBA) mixed-matrix membrane containing 0.1 wt% GO nanosheets and reportedly observed a 100% enhancement in CO_2 permeability without compromising on the CO_2/CH_4 selectivity (Table 1) [54]. At high loadings, however, the graphene-based fillers play a role that is similar to that of the stacked laminates. This was demonstrated by Li et al. who prepared a poly(amide-6-b-ethylene oxide) (Pebax)-based mixed-matrix membrane incorporated with 10 wt% polyethylene glycol- and polyethyleneimine-functionalized GO (PEG-PEI-GO) nanosheets [55]. Accordingly, the high-aspect-ratio of the GO nanosheets generated a tortuous pathway, which favored the diffusion of smaller CO_2 molecules at a lower transport resistance as compared to the larger CH_4 molecules. This result was exemplified by the higher CO_2/CH_4 diffusivity selectivity when PEG-PEI-GO was incorporated.

Another key highlight of the work by Li et al. [55] was the chemical functionalization of GO nanosheets. Chemical functionalization was used in this case to afford an intimate interfacial gap between the GO nanosheets and the Pebax matrix, making the mixed-matrix membrane defect-free. Intrinsically, pristine GO nanosheets already possess hydrophilic oxygen-containing functional groups, such as hydroxyl and carboxyl groups, that are compatible with a number of polymer matrices, including Pebax. To further strengthen their capacity to create an ideal interfacial gap for a multitude of other polymer matrices, grafting GO nanosheets with amine- and amino-based functional groups has become a widely adopted strategy [5,55,56]. This strategy not only improves the compatibility at the GO/polymer interface but the amine- and amino-based groups also increase the CO_2 affinity, leading to an enhanced CO_2 permeability without compromising on the CO_2/CH_4 selectivity. Essentially, such merits are only realizable owing to the tunable physicochemical properties of the graphene-based materials.

Apart from enhancing the CO_2/CH_4 separation performances, graphene-based materials are also well-known for their good mechanical properties [57]. Critically, their use as fillers in mixed-matrix membranes can help to enhance the mechanical properties of the membranes. For example, Li et al. added 10 wt% loading of GO nanosheets in a Matrimid® matrix to demonstrate a >100% increment in Young's modulus of the membrane [58]. Similarly, in another work, a 5 wt% loading of GO nanosheets in a 4,4′-oxydiphthalic anhydride-2,4,6-trimethyl-*m*-phenylenediamine (ODPA-TMPDA) polymer matrix was also able to produce improved tensile strength and Young's modulus by 17% and 3%, respectively [59]. Furthermore, in both works, dual fillers were exploited to create a synergistic effect in the separation performances of the membranes. The ability of GO nanosheets to elevate the mechanical properties of the mixed-matrix membranes, therefore, helps to modulate the drop in the mechanical properties caused by the second filler. As an illustration, 10 wt% ZIF-8 was added to the ODPA-TMPDA membrane and found to reduce the tensile strength and Young's modulus of the membrane by 11% and 8%, respectively. With the incorporation of 5 wt% GO nanosheets alongside 10 wt% loading of ZIF-8, the tensile strength and Young's modulus not only reverted to that of the unfilled ODPA-TMPDA membrane but also slightly improved by 9% and 1%, respectively [59]. Here, it is noteworthy to highlight that the optimal loading of GO nanosheets is polymer- and application-specific. There is no strong indication to suggest a ubiquitously optimal filler loading as evidenced by mixed-matrix membranes of graphene-based or other 2D-layered materials for a variety of applications [60–62]. However, one thing for sure is that as the loading of GO nanosheets gets higher, there runs a higher risk of defective membrane formation as a result of increased difficulties

in dispersing the GO nanosheets. This generally will lead to increased agglomeration of the GO fillers, in which the extent depends on the solvent systems used in the polymer dope solutions.

4.1. Challenges

Compared to the other membrane designed discussed in this article, one of the competitive advantages of graphene-based mixed-matrix membranes is the easy retrofitting and more scalable fabrications given minimal adaptation needed for existing polymer membrane production. Also, mixed-matrix membranes are more cost-competitive as compared to graphene-based stacked laminates due to the smaller amount of graphene-based materials needed, as well as greater reliability in terms of mechanical properties and membrane performances given that the membranes comprise primarily of polymeric materials. Despite that, there are some uncertainties regarding the prospects of graphene-based mixed-matrix membranes for CO_2/CH_4 separation. First, there are limited number of studies on the fabrication of graphene-based hollow fiber mixed-matrix membranes. Among the 32 graphene-based mixed-matrix membranes reviewed thus far (Table 1), only one study by Zahri and coworkers was reported in hollow fiber configurations [63]. Hence, the impact of the graphene-based mixed-matrix membrane design on real industrial application remains unknown. Second, graphene-based materials employed in mixed-matrix membranes appear more useful in elevating the CO_2/CH_4 selectivity of the membranes rather than enhancing the CO_2 permeability. Statistically speaking, among the reviewed membranes, only 66% of them exhibited a positive permeability enhancement, while 81% of them gave a positive selectivity enhancement (Table 1). In addition, there exist conflicting results in the separation performances. For example, Li et al. demonstrated a 107% enhancement in the CO_2/CH_4 selectivity when 10 wt% of GO was loaded into a Matrimid® matrix [58]. However, Castarlenas and coworkers showed otherwise with a 36% decrease in the selectivity when 8 wt% loading of GO was used instead (Table 1) [64]. Hence, there is a need to better understand the role of graphene-based materials and the desirable attributes which they can offer. At this point, we would like to highlight that performance enhancements greater than 100% are not uncommon in the literature. This simply means that the performances are enhanced greater than two times as compared to the unfilled membranes. Third, there is a lack of effective benchmarking of the filler materials for mixed-matrix membranes. Currently, the Robeson upper bound is the benchmark used to evaluate membrane performances (Figure 4a). There are other self-proclaimed upper bounds that were redefined by next-generation materials, composite and mixed-matrix membranes [65]. However, to date, the 2008 upper bound for polymeric membranes remains the most robustly examined upper bound and so is officially recognized as the gold standard. Exceeding the upper bound has since become the holy grail of the academia. This upper bound was initially defined for polymeric membranes only and, except for the seemingly good separation performances, transcending the upper bound does not really tell more about the quality of the filler materials [5]. Hence, we contend that there is a need to supplement the Robeson upper bound with a more specific benchmark that is targeted at mixed-matrix membranes (see reference [5] for our previous arguments).

Table 1. A summary of the carbon dioxide (CO_2)/methane gas (CH_4) separation performance of graphene-based mixed-matrix membranes in the literature.

Filler	Polymer Matrix	Filler Loading (wt%)	Separation Performance							Ref.
			Testing Condition		$P(CO_2)$ (barrer)	Permeability Enhancement (%) [a]	$\alpha(CO_2/CH_4)$	Selectivity Enhancement (%) [a]	F_{index} value	
			Pres. (bar)	Temp. (°C)						
Nonfunctionalized graphene	PDMS	0.5	1.1	37	4460	47.68	4.2	16.67	0.80	[66]
GO	PDMS	1	10	35	2429.76	−40.69	3.58	17.6	−0.10	[67]
GO	PDMS	8	10.1	35	142.22	−60.00	9.40	209.90	2.07	[68]
GO	Pebax 1657	1	3	25	100.00	102.06	24.66	14.42	1.06	[54]
PEI-PEG-GO	Pebax 1657	10	2	30	145.00	76.83	24.0	26.32	1.19	[55]
PEI-PEG-GO	Pebax 1657	10	2	30	1330.00	170.87	45.0	136.84	3.27	[55]
Im-GO	Pebax 1657	0.8	4	25	64.00	3.56	25.10	−3.83	−0.07	[69]
Few-layer graphene	PIM-1	0.00096	1	25	12700	148.05	8.76	−41.84	−0.52	[70]
Few-layer graphene	PIM-1	0.0071	1	25	3410	33.40	21.31	41.53	1.20	[70]
Few-layer graphene	PIM-1 (200-day aging)	0.00096	1	25	9240	151.77	9.43	−48.62	−0.83	[70]
GO	Matrimid®	0.5	0.5	26	76.00	−49.33	21.71	21.6	−0.16	[71]
GO	Matrimid®	2	2	30	11.73	32.69	48.83	43.62	1.24	[58]
GO	Matrimid®	10	2	30	6.46	−26.92	70.30	106.76	1.60	[58]
MWCNT/GO (1:1)	Matrimid®	10	2	30	38.07	330.66	84.60	148.82	3.86	[58]
Graphene	Matrimid®	10	2	30	9.89 [b]	20.76	20.16	−28.6	−0.70	[58]
MWCNT/GO (1:1)	Matrimid®	10	2	30	35.43 [b]	332.60	78.57	178.12	4.16	[58]
GO	PEO-PBTP	0.075	0.5	25	130.00	−13.33	21.70	21.5	0.37	[71]
GO	PEO-PBTP/PAN	0.075	0.5	25	603.07 [c]	−25.00	21.71	18.4	0.16	[71]
GO	PEO-PBTP/PAN	0.5	0.5	25	241.23 [c]	−70.00	21.29	16.1	−0.81	[71]
GO	Matrimid®	8	3.4	35	3.89	−47.07	20.50	−36.34	−1.83	[72]
GO	PSF	8	3.4	35	2.98	−51.70	16.67	−45.34	−2.32	[72]
MWCNT/GO nanoribbons	PI	1	1	35	17	13.3	25.0	92.3	1.85	[73]
Da-Cys-GO	SPEEK	8	1.5	25	22.26	43.87	48.8	82.77	1.95	[56]
Da-Cys-GO	SPEEK	8	1	25	1247.60	120.70	81.8	207.52	3.75	[56]
Da-Cys-GO	SPEEK	8	1	25	1227.00 [b]	117.05	80.7	203.38	3.70	[56]
GO	ODPA-TMPDA	5	1	25	98.51 [d]	7.49	41.10	29.58	0.76	[59]
ZIF-8/GO (1:2)	ODPA-TMPDA	5	1	25	146.57 [d]	60.00	40.92	29.01	1.14	[59]
GO	Matrimid®	10	1	25	7.28 [d]	–27.38	45.61	24.20	0.25	[74]
NiDOBDC/GO (1:1)	Matrimid®	10	1	25	10.34 [d]	3.57	49.93	35.97	0.85	[74]
Graphene	PSF	0	5	25	86.80 [c]	34.64	25.98	35.31	1.09	[63]
GO	Pebax	0.25	5	35	8.44 [c]	–21.92	13.89	83.00	1.35	[14]
GO	Pebax/PEG (1/1)	0.25	5	35	11.98 [c]	10.82	14.02	84.72	1.72	[14]

PEI: polyethyleneimine, PEG: polyethylene glycol; Im: imidazole; MWCNT: multi-walled carbon nanotube; Da: dopamine; Cys: cysteine; PDMS: polydimethylsiloxane; Pebax: poly(amide-6-*b*-ethylene oxide); PEO-PBTP: poly(ethylene oxide)-poly(butylene terephthalate); PSf: polysulfone; PI: polyimide; SPEEK: sulfonated poly(ether ether ketone); ODPA-TMPDA: 4,4′-oxydiphthalic anhydride-2,4,6-trimethyl-*m*-phenylenediamine; PAN: polyacrylonitrile. [a] Permeability enhancements are calculated by taking the difference between the permeability of the mixed-matrix membranes and unfilled membranes divided by the permeability of the unfilled membranes and converting the values as percentages. The same method was also applied for selectivity enhancements. [b] Performance evaluated under CO_2/CH_4 mixed gas feed of 30/70 CO_2/CH_4. [c] Asymmetric membranes with $P(CO_2)$ reported as permeance with units of GPU. [d] Performance evaluated under CO_2/CH_4 mixed gas feed of 50/50 CO_2/CH_4.

4.2. Perspectives

To address the above challenges, our group had recently derived an empirical filler enhancement index known as the F_{index} to offer a new approach in quantifying and evaluating the effectiveness of filler materials in the mixed-matrix membranes (see Reference [5] for the full derivation of the F_{index}). This is realized by normalizing the CO_2 permeability and CO_2/CH_4 selectivity of the mixed-matrix membrane by the unfilled polymeric membrane. As a result, the effect brought by the polymer matrix is decoupled to better illuminate the impact brought by the filler materials. The F_{index} is defined as follows:

$$F_{\text{index}} = \ln\left(\frac{P_{composite}}{P_{unfilled}}\right) + 2.636\ln\left(\frac{\alpha_{composite}}{\alpha_{unfilled}}\right), \quad (1)$$

where $P_{composite}$ and $P_{unfilled}$, in this context, refer to the CO_2 permeability of the graphene-based mixed-matrix and unfilled membranes, respectively. The $\alpha_{composite}$ and $\alpha_{unfilled}$ refer to the CO_2/CH_4 selectivity of the graphene-based mixed-matrix membranes and unfilled membranes, respectively.

The F_{index} is a composite metric which encompasses both the permeability and selectivity enhancement terms, making comparison of the effectiveness of graphene-based fillers more accurate, holistic and straightforward. For example, when 0.25 wt% of GO nanosheets were incorporated into a Pebax matrix, the CO_2 permeability decreased by 22% but the selectivity was enhanced by 83% [14]. But, when 0.8 wt% of imidazole-functionalized GO (Im-GO) nanosheets were incorporated into the Pebax matrix, the CO_2 permeability instead increased, while the selectivity decreased by 4%, respectively [69]. Here, to judge that the GO nanosheets were more effective than the Im-GO or vice versa was rather contentious. This is because there is a need to grapple with two terms and this has made effectiveness evaluation of graphene-based filler sometimes contradicting. With F_{index}, however, such controversy is non-existent. By integrating the two terms into one single rating, the metric and thus filler effectiveness evaluation is easier to understand and implement. In this case, GO nanosheets scored a F_{index} value of 1.35, while Im-GO nanosheets had a value of −0.07, making GO a more effective filler than Im-GO for the Pebax matrix. The F_{index} is also formulated to give a stronger emphasis on the selectivity enhancement by amplifying the term with an enhancement coefficient of 2.636, which is the upper bound slope of the 2008 CO_2/CH_4 Robeson plot [75]. This is to recognize filler materials that have the capacity to enhance the CO_2/CH_4 selectivity. At the same time, through emphasizing the selectivity enhancement, we can discredit filler materials that enhance gas permeability at the expense of membrane selectivity, which is commonly associated with membrane defects or nonidealities formation. Furthermore, with the integration of the enhancement coefficient, the F_{index} is demonstrated to be accurate and reliable as evidenced by its ability to identify the top 20 filler materials out of a database with 470 sample size (Figure 4b–d and see reference [5]). However, the F_{index} is yet to be perfected [5]. For example, critical qualities including polymer/filler compatibilities, mechanical properties, physical aging effects should ideally be taken into account [76–78]. But, unlike separation performance data which are fervently documented, data of these qualities are scarce and hard to quantify, making the feat of perfecting the F_{index} challenging.

In the process of developing the F_{index}, the F_{index} values were also empirically categorized into five different labels to give meaningful interpretations of the fillers. The filler labels, namely, (1) ideal, (2) exemplary, (3) competent, (4) moderate, and (5) inadequate, were created to cover F_{index} values of >8.00, 8.00–4.00, 4.00–1.50, 1.50–0.00, and <0.00, respectively. To date, no filler has achieved the highest accolade of the ideal label [5]. Among the surveyed graphene-based fillers, 31% of them achieved a label of either exemplary or competent, while 41% and 28% achieved a moderate and inadequate label, respectively. These accomplishments are slightly less stellar than the metal-organic frameworks (MOFs), which are also prominently used as fillers in mixed-matrix membranes [5]. Among the 148 MOF fillers surveyed thus far [5], 36% of them has a label of either exemplary or competent and 51% obtain a moderate label. Only 13% of the MOFs is labelled inadequate. Although the figures are less compelling, we believe that graphene-based fillers can add value in their own ways. One of them is to utilize the 2D morphology of graphene-based fillers to enhance the membrane selectivity polymeric

matrices with high intrinsic permeability. Typically, one of the drawbacks of polymers with high intrinsic permeability, such as PIM-1 and 6FDA-based polymers, is the low CO_2/CH_4 selectivity [79]. By using graphene-based fillers to enhance the selectivity while sacrificing the CO_2 permeability to a limited extent, it will be easier to realize high-performance mixed-matrix membranes that surpass the 2008 Robeson upper bound.

In this respect, we foresee that the F_{index} will be able to empower researchers with higher competencies in making data-driven decisions for designing mixed-matrix membranes. Explicitly, this entails leveraging the F_{index} values of specific graphene-based materials to help match with suitable polymer matrices of the right intrinsic separation performances so as to elicit the ideal polymer/filler pair that best optimize the performances of the mixed-matrix membranes. Furthermore, with this ability to align graphene-based filler materials with polymer matrices, it will also help accelerate the translation of flat-sheet to hollow fiber graphene-based mixed-matrix membranes, as well as the development of more complex membrane designs, such as the thin-film nanocomposite membranes where graphene-based materials are incorporated into the thin selective layer of the membranes (Figure 4e), and which is of particular interest. We believe that by strategically optimizing membrane design from a data-driven approach, high-performance graphene-based thin-film nanocomposite membranes, especially those in the hollow fiber configuration, can be realized. This will be a game-changer, considering that the amount of graphene-based materials used will be relatively lower than the mixed-matrix membranes and this will give a low-cost competitive advantage over all the other membrane designs discussed in this article [80].

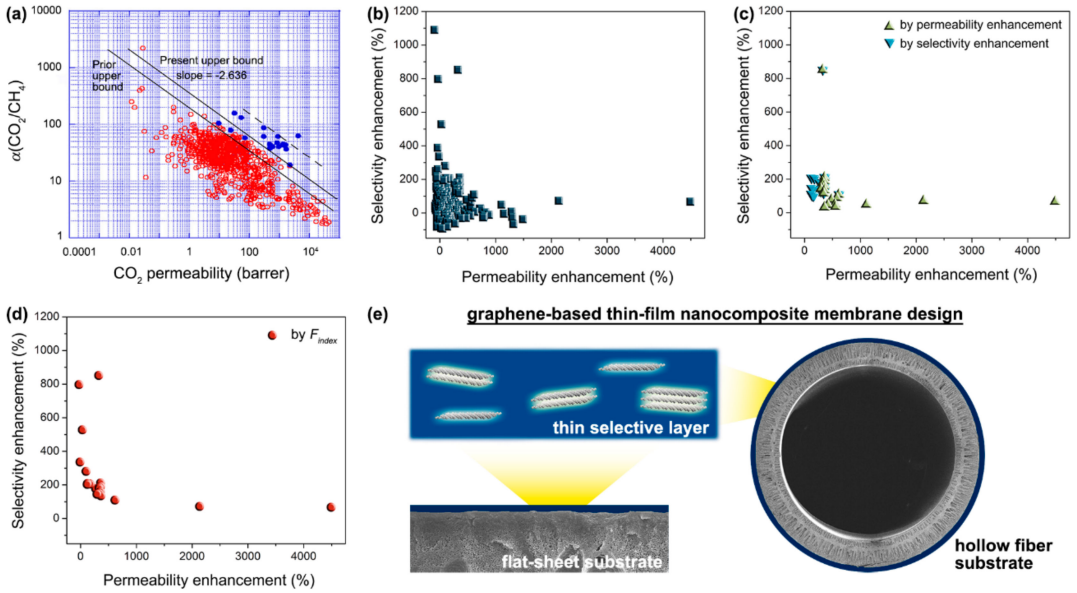

Figure 4. (**a**) CO_2/CH_4 Robeson plot showing the prior upper bound (1991) and the present upper bound (2008) with a slope of –2.636. Adapted from Reference [75]. (**b**) The performance plot of 470 filler materials surveyed to date, showing their selectivity enhancement as a function of their permeability enhancement. (**c**) Top 20 fillers selected based on their permeability and selectivity enhancements. (**d**) Top 20 fillers selected based on their F_{index} values with outstanding performance enhancements accurately singled out from Figure 4b. Adapted from Reference [5]. (**e**) Schematic illustration of the graphene-based thin-film nanocomposite membranes with both flat-sheet and hollow fiber configurations. Creative Commons license CC BY 4.0.

5. Conclusions

In this short paper, we have provided a succinct summary of the current status of nanoporous single-layer graphene, few- to multi-layer graphene-based stacked laminates, and mixed-matrix membranes with an emphasis towards CO_2/CH_4 separation. Notably, the major challenges faced

by each membrane design, as well as key insights and proposed solutions, are put into perspective. In essence, nanoporous single-layer graphene membranes boast the highest separation performances, owing to the monoatomic thickness, and thus they have the lowest conceptual transport resistance of a single-layer graphene. However, the low scalability and high cost of production will continue to plague this type of membrane design. Few- to multi-layer graphene-based stacked laminates as membranes for CO_2/CH_4 separation appear to be more technically scalable and exhibit reasonably good performances. Yet, the cost of production is likely to remain higher than mixed-matrix and current polymeric membranes. Also, literature reports are scarce in terms of the hollow fiber stacked laminates aimed at CO_2/CH_4 separation, rendering the relevance and feasibility of this membrane design for industrial application indefinite. At present, graphene-based mixed-matrix membranes, including the hollow fiber membrane configuration, have the highest commercial value given the relative ease of fabrication and scalability potential. The challenge lies in deepening our understanding of the real impact brought by the graphene-based materials and how to realize optimized mixed-matrix membranes by matching the right polymer matrix to the graphene-based material to achieve maximized separation performances. For this purpose, we recommend a data-driven approach using a newly developed F_{index} to help enhance decision-making competencies of researchers, as well as to use it as a benchmark to complement the current Robeson upper bound. Overall, from a big picture standpoint, we map out the current technology landscape of graphene-based membranes from three aspects: (1) separation performance enhancement, (2) commercial viability that includes scalability and mechanical robustness, as well as industrial relevance, and (3) production cost (Figure 5). Apparently, nanoporous single-layer graphene stands at the top of the plot, while conventional polymeric membranes take the opposite end. Graphene-based stacked laminates are likely to be in the center of the plot given the higher technical difficulties in large-scale fabrications and the lack of rigorous techno-economic analysis. Obviously, mixed-matrix and thin-film nanocomposite membranes are positioned in between the stacked laminates and conventional polymeric membranes (Figure 5). Pushing beyond these efforts, we believe that optimizing graphene-based mixed-matrix and thin-film nanocomposite membranes (in particular hollow fiber membranes) by leveraging data analytics will not only open up more compelling opportunities to elevate membrane-based CO_2/CH_4 separation but also reduce risk to a level that is appealing to the industry and for ensuring commercial success.

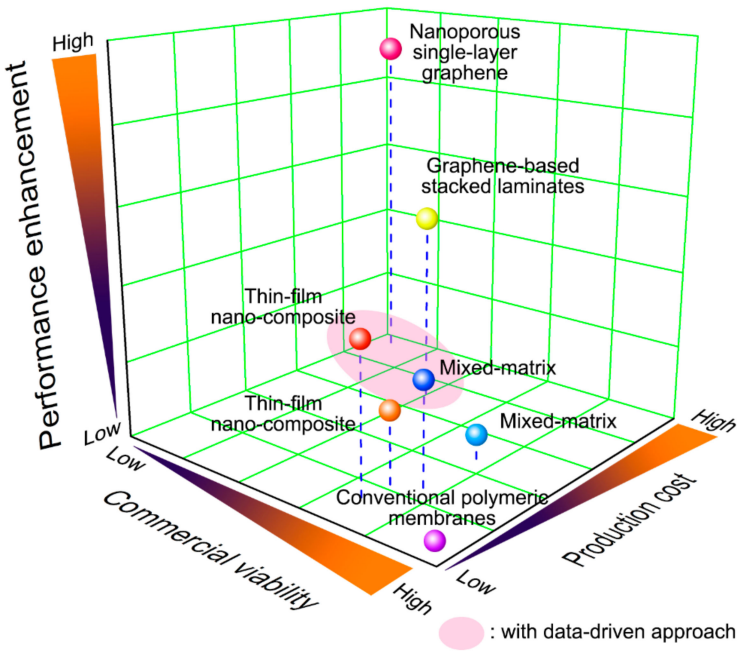

Figure 5. A projected outlook of graphene-based membranes for CO_2/CH_4 separation.

Author Contributions: K.G. conceptualized this paper and drafted the original manuscript. H.E.K., E.Y. and T.-H.B. reviewed and edited the manuscript, analyzed critical data used and provided invaluable insights to the discussion.

Funding: This research received no external funding.

Acknowledgments: The authors would like to thank the Singapore Economic Development Board for its funding support to Singapore Membrane Technology Centre.

Conflicts of Interest: The authors declare no conflict of interest.

References

1. Connor, P.; Cleveland, C.U.S. Energy Transitions 1780–2010. *Energies* **2014**, *7*, 7955–7993. [CrossRef]
2. Holmes, D.E.; Smith, J.A. Chapter One—Biologically Produced Methane as a Renewable Energy Source. *Adv. Appl. Microbiol.* **2016**, *97*, 1–61. [PubMed]
3. Geppert, F.; Liu, D.; van Eerten-Jansen, M.; Weidner, E.; Buisman, C.; Ter Heijne, A. Bioelectrochemical Power-to-Gas: State of the Art and Future Perspectives. *Trends Biotechnol.* **2016**, *34*, 879–894. [CrossRef] [PubMed]
4. Baker, R.W.; Lokhandwala, K. Natural gas processing with membranes: An overview. *Ind. Eng. Chem. Res.* **2008**, *47*, 2109–2121. [CrossRef]
5. Chuah, C.Y.; Goh, K.; Yang, Y.; Gong, H.; Li, W.; Karahan, H.E.; Guiver, M.D.; Wang, R.; Bae, T.-H. Harnessing Filler Materials for Enhancing Biogas Separation Membranes. *Chem. Rev.* **2018**, *118*, 8655–8769. [CrossRef] [PubMed]
6. Dumee, L.; Scholes, C.; Stevens, G.; Kentish, S. Purification of aqueous amine solvents used in post combustion CO_2 capture: A review. *Int. J. Greenh. Gas Control* **2012**, *10*, 443–455. [CrossRef]
7. Zhang, Y.; Sunarso, J.; Liu, S.; Wang, R. Current status and development of membranes for CO_2/CH_4 separation: A review. *Int. J. Greenh. Gas Control* **2013**, *12*, 84–107. [CrossRef]
8. Xu, Q.; Xu, H.; Chen, J.; Lv, Y.; Dong, C.; Sreeprasad, T.S. Graphene and graphene oxide: Advanced membranes for gas separation and water purification. *Inorg. Chem. Front.* **2015**, *2*, 417–424. [CrossRef]
9. Liu, G.; Jin, W.; Xu, N. Graphene-based membranes. *Chem. Soc. Rev.* **2015**, *44*, 5016–5030. [CrossRef]
10. Celebi, K.; Buchheim, J.; Wyss, R.M.; Droudian, A.; Gasser, P.; Shorubalko, I.; Kye, J.-I.; Lee, C.; Park, H.G. Ultimate Permeation Across Atomically Thin Porous Graphene. *Science* **2014**, *344*, 289–292. [CrossRef]
11. Goh, K.; Karahan, H.E.; Wei, L.; Bae, T.H.; Fane, A.G.; Wang, R.; Chen, Y. Carbon Nanomaterials for Advancing Separation Membranes: A Strategic Perspective. *Carbon* **2016**, *109*, 694–710. [CrossRef]
12. Goh, K.; Setiawan, L.; Wei, L.; Si, R.; Fane, A.G.; Wang, R.; Chen, Y. Graphene oxide as effective selective barriers on a hollow fiber membrane for water treatment process. *J. Membr. Sci.* **2015**, *474*, 244–253. [CrossRef]
13. Goh, K.; Heising, J.K.; Yuan, Y.; Karahan, H.E.; Wei, L.; Zhai, S.; Koh, J.X.; Htin, N.M.; Zhang, F.; Wang, R.; et al. Sandwich-Architectured Poly(lactic acid)-Graphene Composite Food Packaging Films. *ACS Appl. Mater. Interfaces* **2016**, *8*, 9994–10004. [CrossRef] [PubMed]
14. Norahim, N.; Kajornsak, F.; Quitain, A.T.; Klaysom, C. Composite membranes of graphene oxide for CO_2/CH_4 separation. *J. Chem. Technol. Biotechnol.* **2019**. [CrossRef]
15. Galizia, M.; Chi, W.S.; Smith, Z.P.; Merkel, T.C.; Baker, R.W.; Freeman, B.D. 50th Anniversary Perspective: Polymers and Mixed Matrix Membranes for Gas and Vapor Separation: A Review and Prospective Opportunities. *Macromolecules* **2017**, *50*, 7809–7843. [CrossRef]
16. Ali, A.; Pothu, R.; Siyal, S.H.; Phulpoto, S.; Sajjad, M.; Thebo, K.H. Graphene-based membranes for CO_2 separation. *Mater. Sci. Energy Technol.* **2019**, *2*, 83–88. [CrossRef]
17. Werber, J.R.; Osuji, C.O.; Elimelech, M. Materials for next-generation desalination and water purification membranes. *Nat. Rev. Mater.* **2016**, *1*, 16018. [CrossRef]
18. Hegab, H.M.; Zou, L. Graphene oxide-assisted membranes: Fabrication and potential applications in desalination and water purification. *J. Membr. Sci.* **2015**, *484*, 95–106. [CrossRef]
19. Yoo, B.M.; Shin, H.-J.; Yoon, H.W.; Park, H.B. Graphene and graphene oxide and their uses in barrier polymers. *J. Appl. Polym. Sci.* **2014**, *131*, 39628. [CrossRef]
20. Bunch, J.S.; Verbridge, S.S.; Alden, J.S.; van der Zande, A.M.; Parpia, J.M.; Craighead, H.G.; McEuen, P.L. Impermeable Atomic Membranes from Graphene Sheets. *Nano Lett.* **2008**, *8*, 2458–2462. [CrossRef]

21. O'Hern, S.C.; Boutilier, M.S.H.; Idrobo, J.-C.; Song, Y.; Kong, J.; Laoui, T.; Atieh, M.; Karnik, R. Selective Ionic Transport through Tunable Subnanometer Pores in Single-Layer Graphene Membranes. *Nano Lett.* **2014**, *14*, 1234–1241. [CrossRef] [PubMed]
22. Gethers, M.L.; Thomas, J.C.; Jiang, S.; Weiss, N.O.; Duan, X.; Goddard, W.A. III.; Weiss, P.S. Holey Graphene as a Weed Barrier for Molecules. *ACS Nano* **2015**, *9*, 10909–10915. [CrossRef] [PubMed]
23. Surwade, S.P.; Smirnov, S.N.; Vlassiouk, I.V.; Unocic, R.R.; Veith, G.M.; Dai, S.; Mahurin, S.M. Water desalination using nanoporous single-layer graphene. *Nat. Nanotechnol.* **2015**, *10*, 459–464. [CrossRef] [PubMed]
24. Zhao, J.; He, G.; Huang, S.; Villalobos, L.F.; Dakhchoune, M.; Bassas, H.; Agrawal, K.V. Etching gas-sieving nanopores in single-layer graphene with an angstrom precision for high-performance gas mixture separation. *Sci. Adv.* **2019**, *5*, eaav1851. [CrossRef] [PubMed]
25. Koenig, S.P.; Wang, L.D.; Pellegrino, J.; Bunch, J.S. Selective molecular sieving through porous graphene. *Nat. Nanotechnol.* **2012**, *7*, 728–732. [CrossRef] [PubMed]
26. Bartolomei, M.; Carmona-Novillo, E.; Hernández, M.I.; Campos-Martínez, J.; Pirani, F.; Giorgi, G. Graphdiyne Pores: "Ad Hoc" Openings for Helium Separation Applications. *J. Phys. Chem. C* **2014**, *118*, 29966–29972. [CrossRef]
27. Li, Y.; Xu, L.; Liu, H.; Li, Y. Graphdiyne and graphyne: From theoretical predictions to practical construction. *Chem. Soc. Rev.* **2014**, *43*, 2572–2586. [CrossRef]
28. Gao, X.; Liu, H.; Wang, D.; Zhang, J. Graphdiyne: Synthesis, properties, and applications. *Chem. Soc. Rev.* **2019**, *48*, 908–936. [CrossRef]
29. Jiao, Y.; Du, A.; Hankel, M.; Zhu, Z.; Rudolph, V.; Smith, S.C. Graphdiyne: A versatile nanomaterial for electronics and hydrogen purification. *Chem. Commun.* **2011**, *47*, 11843–11845. [CrossRef]
30. Bae, S.; Kim, H.; Lee, Y.; Xu, X.; Park, J.-S.; Zheng, Y.; Balakrishnan, J.; Lei, T.; Ri Kim, H.; Song, Y.I.; et al. Roll-to-roll production of 30-inch graphene films for transparent electrodes. *Nat. Nanotechnol.* **2010**, *5*, 574. [CrossRef]
31. Shivayogimath, A.; Whelan, P.R.; Mackenzie, D.M.A.; Luo, B.; Huang, D.; Luo, D.; Wang, M.; Gammelgaard, L.; Shi, H.; Ruoff, R.S.; et al. Do-It-Yourself Transfer of Large-Area Graphene Using an Office Laminator and Water. *Chem. Mater.* **2019**, *31*, 2328–2336. [CrossRef]
32. Li, H.; Song, Z.; Huang, Y.; Li, S.; Mao, Y.; Ploehn, H.J.; Bao, Y.; Yu, M. Ultrathin, Molecular-Sieving Graphene Oxide Membranes for Selective Hydrogen Separation. *Science* **2013**, *342*, 95–98. [CrossRef] [PubMed]
33. Wang, S.F.; Wu, Y.Z.; Zhang, N.; He, G.W.; Xin, Q.P.; Wu, X.Y.; Wu, H.; Cao, X.Z.; Guiver, M.D.; Jiang, Z.Y. A highly permeable graphene oxide membrane with fast and selective transport nanochannels for efficient carbon capture. *Energy Environ. Sci.* **2016**, *9*, 3107–3112. [CrossRef]
34. Goh, K.; Jiang, W.C.; Karahan, H.E.; Zhai, S.L.; Wei, L.; Yu, D.S.; Fane, A.G.; Wang, R.; Chen, Y. All-Carbon Nanoarchitectures as High-Performance Separation Membranes with Superior Stability. *Adv. Funct. Mater.* **2015**, *25*, 7348–7359. [CrossRef]
35. Shen, J.; Liu, G.; Huang, K.; Chu, Z.; Jin, W.; Xu, N. Subnanometer Two-Dimensional Graphene Oxide Channels for Ultrafast Gas Sieving. *ACS Nano* **2016**, *10*, 3398–3409. [CrossRef] [PubMed]
36. Kim, H.W.; Yoon, H.W.; Yoon, S.-M.; Yoo, B.M.; Ahn, B.K.; Cho, Y.H.; Shin, H.J.; Yang, H.; Paik, U.; Kwon, S.; et al. Selective Gas Transport Through Few-Layered Graphene and Graphene Oxide Membranes. *Science* **2013**, *342*, 91–95. [CrossRef] [PubMed]
37. Chen, L.; Moon, J.-H.; Ma, X.; Zhang, L.; Chen, Q.; Chen, L.; Peng, R.; Si, P.; Feng, J.; Li, Y.; et al. High performance graphene oxide nanofiltration membrane prepared by electrospraying for wastewater purification. *Carbon* **2018**, *130*, 487–494. [CrossRef]
38. Akbari, A.; Sheath, P.; Martin, S.T.; Shinde, D.B.; Shaibani, M.; Banerjee, P.C.; Tkacz, R.; Bhattacharyya, D.; Majumder, M. Large-area graphene-based nanofiltration membranes by shear alignment of discotic nematic liquid crystals of graphene oxide. *Nat. Commun.* **2016**, *7*, 10891. [CrossRef]
39. Yang, Y.-H.; Bolling, L.; Priolo, M.A.; Grunlan, J.C. Super Gas Barrier and Selectivity of Graphene Oxide-Polymer Multilayer Thin Films. *Adv. Mater.* **2013**, *25*, 503–508. [CrossRef]
40. Gadipelli, S.; Guo, Z.X. Graphene-based materials: Synthesis and gas sorption, storage and separation. *Prog. Mater. Sci.* **2015**, *69*, 1–60. [CrossRef]

41. Khakpay, A.; Rahmani, F.; Nouranian, S.; Scovazzo, P. Molecular Insights on the CH_4/CO_2 Separation in Nanoporous Graphene and Graphene Oxide Separation Platforms: Adsorbents versus Membranes. *J. Phys. Chem. C* **2017**, *121*, 12308–12320. [CrossRef]
42. Wang, S.; Xie, Y.; He, G.; Xin, Q.; Zhang, J.; Yang, L.; Li, Y.; Wu, H.; Zhang, Y.; Guiver, M.D.; et al. Graphene Oxide Membranes with Heterogeneous Nanodomains for Efficient CO_2 Separations. *Angew. Chem. Int. Ed.* **2017**, *56*, 14246–14251. [CrossRef] [PubMed]
43. Ren, Y.; Peng, D.; Wu, H.; Yang, L.; Wu, X.; Wu, Y.; Wang, S.; Jiang, Z. Enhanced carbon dioxide flux by catechol–Zn^{2+} synergistic manipulation of graphene oxide membranes. *Chem. Eng. Sci.* **2019**, *195*, 230–238. [CrossRef]
44. Fam, W.; Mansouri, J.; Li, H.; Hou, J.; Chen, V. Gelled Graphene Oxide–Ionic Liquid Composite Membranes with Enriched Ionic Liquid Surfaces for Improved CO_2 Separation. *ACS Appl. Mater. Interfaces* **2018**, *10*, 7389–7400. [CrossRef] [PubMed]
45. Liu, C.; Greer, D.W.; O'Leary, B.W. Advanced Materials and Membranes for Gas Separations: The UOP Approach. In *Nanotechnology: Delivering on the Promise Volume 2*; American Chemical Society: Washington, WA, USA, 2016; pp. 119–135. [CrossRef]
46. Baker, R.W. *Membrane Technology and Applications*, 2nd ed.; John Wiley & Sons, Ltd.: Hoboken, NJ, USA, 2004; pp. 1–538.
47. Chen, L.; Li, Y.; Chen, L.; Li, N.; Dong, C.; Chen, Q.; Liu, B.; Ai, Q.; Si, P.; Feng, J.; et al. A large-area free-standing graphene oxide multilayer membrane with high stability for nanofiltration applications. *Chem. Eng. J.* **2018**, *345*, 536–544. [CrossRef]
48. Chen, X.Y.; Vinh-Thang, H.; Ramirez, A.A.; Rodrigue, D.; Kaliaguine, S. Membrane gas separation technologies for biogas upgrading. *Rsc. Adv.* **2015**, *5*, 24399–24448. [CrossRef]
49. Shah, M.S.; Tsapatsis, M.; Siepmann, J.I. Hydrogen Sulfide Capture: From Absorption in Polar Liquids to Oxide, Zeolite, and Metal-Organic Framework Adsorbents and Membranes. *Chem. Rev.* **2017**, *117*, 9755–9803. [CrossRef]
50. Baker, R.W. Future directions of membrane gas separation technology. *Ind. Eng. Chem. Res.* **2002**, *41*, 1393–1411. [CrossRef]
51. Scholz, M. Membrane based Biogas Upgrading Processes. Ph.D. Thesis, RWTH Aachen University, Aachen, Germany, 2013.
52. Cheng, Y.; Wang, Z.; Zhao, D. Mixed Matrix Membranes for Natural Gas Upgrading: Current Status and Opportunities. *Ind. Eng. Chem. Res.* **2018**, *57*, 4139–4169. [CrossRef]
53. Noble, R.D. Perspectives on mixed matrix membranes. *J. Membr. Sci.* **2011**, *378*, 393–397. [CrossRef]
54. Shen, J.; Liu, G.; Huang, K.; Jin, W.; Lee, K.R.; Xu, N. Membranes with Fast and Selective Gas-Transport Channels of Laminar Graphene Oxide for Efficient CO_2 Capture. *Angew. Chem. Int. Ed.* **2015**, *54*, 578–582. [CrossRef]
55. Li, X.; Cheng, Y.; Zhang, H.; Wang, S.; Jiang, Z.; Guo, R.; Wu, H. Efficient CO_2 Capture By Functionalized Graphene Oxide Nanosheets as Fillers to Fabricate Multi-Permselective Mixed Matrix Membranes. *ACS Appl. Mater. Interfaces* **2015**, *7*, 5528–5537. [CrossRef] [PubMed]
56. Xin, Q.; Li, Z.; Li, C.; Wang, S.; Jiang, Z.; Wu, H.; Zhang, Y.; Yang, J.; Cao, X. Enhancing the CO_2 separation performance of composite membranes by the incorporation of amino acid-functionalized graphene oxide. *J. Mater. Chem. A* **2015**, *3*, 6629–6641. [CrossRef]
57. Papageorgiou, D.G.; Kinloch, I.A.; Young, R.J. Mechanical properties of graphene and graphene-based nanocomposites. *Prog. Mater. Sci.* **2017**, *90*, 75–127. [CrossRef]
58. Li, X.Q.; Ma, L.; Zhang, H.Y.; Wang, S.F.; Jiang, Z.Y.; Guo, R.L.; Wu, H.; Cao, X.Z.; Yang, J.; Wang, B.Y. Synergistic effect of combining carbon nanotubes and graphene oxide in mixed matrix membranes for efficient CO_2 separation. *J. Membr. Sci.* **2015**, *479*, 1–10. [CrossRef]
59. Li, W.; Samarasinghe, S.A.S.C.; Bae, T.-H. Enhancing CO_2/CH_4 separation performance and mechanical strength of mixed-matrix membrane via combined use of graphene oxide and ZIF-8. *J. Ind. Eng. Chem.* **2018**, *67*, 156–163. [CrossRef]
60. García-Cruz, L.; Casado-Coterillo, C.; Irabien, Á.; Montiel, V.; Iniesta, J. High Performance of Alkaline Anion-Exchange Membranes Based on Chitosan/Poly (vinyl) Alcohol Doped with Graphene Oxide for the Electrooxidation of Primary Alcohols. *C* **2016**, *2*, 10. [CrossRef]

61. Sánchez-González, S.; Diban, N.; Urtiaga, A. Hydrolytic Degradation and Mechanical Stability of Poly(ε-Caprolactone)/Reduced Graphene Oxide Membranes as Scaffolds for In Vitro Neural Tissue Regeneration. *Membranes* **2018**, *8*, 12. [CrossRef]
62. Marcos-Madrazo, A.; Casado-Coterillo, C.; García-Cruz, L.; Iniesta, J.; Simonelli, L.; Sebastián, V.; Encabo-Berzosa, M.D.M.; Arruebo, M.; Irabien, Á. Preparation and Identification of Optimal Synthesis Conditions for a Novel Alkaline Anion-Exchange Membrane. *Polymers* **2018**, *10*, 913. [CrossRef]
63. Zahri, K.; Goh, P.; Ismail, A. The incorporation of graphene oxide into polysulfone mixed matrix membrane for CO_2/CH_4 separation. *IOP Conf. Ser. Earth Environ. Sci.* **2016**, *36*, 012007. [CrossRef]
64. Castarlenas, S.; Gorgojo, P.; Casado-Coterillo, C.; Masheshwari, S.; Tsapatsis, M.; Téllez, C.; Coronas, J. Melt compounding of swollen titanosilicate JDF-L1 with polysulfone to obtain mixed matrix membranes for H_2/CH_4 separation. *Ind. Eng. Chem. Res.* **2013**, *52*, 1901–1907. [CrossRef]
65. Swaidan, R.; Ghanem, B.; Pinnau, I. Fine-Tuned Intrinsically Ultramicroporous Polymers Redefine the Permeability/Selectivity Upper Bounds of Membrane-Based Air and Hydrogen Separations. *ACS Macro Lett.* **2015**, *4*, 947–951. [CrossRef]
66. Berean, K.J.; Ou, J.Z.; Nour, M.; Field, M.R.; Alsaif, M.M.Y.A.; Wang, Y.C.; Ramanathan, R.; Bansal, V.; Kentish, S.; Doherty, C.M.; et al. Enhanced Gas Permeation through Graphene Nanocomposites. *J. Phys. Chem. C* **2015**, *119*, 13700–13712. [CrossRef]
67. Ha, H.; Park, J.; Ha, K.; Freeman, B.D.; Ellison, C.J. Synthesis and gas permeability of highly elastic poly(dimethylsiloxane)/graphene oxide composite elastomers using telechelic polymers. *Polymer* **2016**, *93*, 53–60. [CrossRef]
68. Ha, H.; Park, J.; Ando, S.; Kim, C.B.; Nagai, K.; Freeman, B.D.; Ellison, C.J. Gas Permeation and Selectivity of Poly(dimethylsiloxane)/Graphene Oxide Composite Elastomer Membranes. *J. Membr. Sci.* **2016**, *518*, 131–140. [CrossRef]
69. Dai, Y.; Ruan, X.H.; Yan, Z.J.; Yang, K.; Yu, M.; Li, H.; Zhao, W.; He, G.H. Imidazole functionalized graphene oxide/PEBAX mixed matrix membranes for efficient CO_2 capture. *Sep. Purif. Technol.* **2016**, *166*, 171–180. [CrossRef]
70. Althumayri, K.; Harrison, W.J.; Shin, Y.; Gardiner, J.M.; Casiraghi, C.; Budd, P.M.; Bernardo, P.; Clarizia, G.; Jansen, J.C. The influence of few-layer graphene on the gas permeability of the high-free-volume polymer PIM-1. *Phil. Trans. R. Soc. A* **2016**, *374*, 1–9. [CrossRef]
71. Karunakaran, M.; Shevate, R.; Kumar, M.; Peinemann, K.V. CO_2-Selective PEO-PBT (PolyActive)/Graphene Oxide Composite Membranes. *Chem. Commun.* **2015**, *51*, 14187–14190. [CrossRef]
72. Castarlenas, S.; Tellez, C.; Coronas, J. Gas separation with mixed matrix membranes obtained from MOF UiO-66-graphite oxide hybrids. *J. Membr. Sci.* **2017**, *526*, 205–211. [CrossRef]
73. Xue, Q.; Pan, X.; Li, X.; Zhang, J.; Guo, Q. Effective enhancement of gas separation performance in mixed matrix membranes using core/shell structured multi-walled carbon nanotube/graphene oxide nanoribbons. *Nanotechnology* **2017**, *28*, 065702. [CrossRef]
74. Li, W.; Chuah, C.Y.; Nie, L.; Bae, T.-H. Enhanced CO_2/CH_4 selectivity and mechanical strength of mixed-matrix membrane incorporated with NiDOBDC/GO composite. *J. Ind. Eng. Chem.* **2019**, *74*, 118–125. [CrossRef]
75. Robeson, L.M. The upper bound revisited. *J. Membr. Sci.* **2008**, *320*, 390–400. [CrossRef]
76. Casado-Coterillo, C.; Del Mar López-Guerrero, M.; Irabien, Á. Synthesis and Characterisation of ETS-10/Acetate-based Ionic Liquid/Chitosan Mixed Matrix Membranes for CO_2/N_2 Permeation. *Membranes* **2014**, *4*, 287–301. [CrossRef] [PubMed]
77. Casado-Coterillo, C.; Fernández-Barquín, A.; Valencia, S.; Irabien, Á. Estimating CO_2/N_2 Permselectivity through Si/Al = 5 Small-Pore Zeolites/PTMSP Mixed Matrix Membranes: Influence of Temperature and Topology. *Membranes* **2018**, *8*, 32. [CrossRef] [PubMed]
78. Yang, Y.; Goh, K.; Weerachanchai, P.; Bae, T.-H. 3D covalent organic framework for morphologically induced high-performance membranes with strong resistance toward physical aging. *J. Membr. Sci.* **2019**, *574*, 235–242. [CrossRef]

79. Wang, S.F.; Li, X.Q.; Wu, H.; Tian, Z.Z.; Xin, Q.P.; He, G.W.; Peng, D.D.; Chen, S.L.; Yin, Y.; Jiang, Z.Y.; et al. Advances in high permeability polymer-based membrane materials for CO_2 separations. *Energy Environ. Sci.* **2016**, *9*, 1863–1890. [CrossRef]
80. Pinnau, I.; Novel Ultra-Microporous Polymers and Thin-film Composite Membranes with Unprecedented Properties for Energy-Efficient Gas Separations. Invited Lecture Singapore Membrane Technology Centre, Singapore. Private communication, 2017.